

2021 Imaging Optics Course Notes - 8

Wide field microscopy of 3D objects

In our discussion about imaging systems we found that the limit on the transverse (x-y) resolution is due to the finite aperture of the lens. For a square aperture in a simple lens imaging system the limit was $\lambda z_2 / B$ in each direction where z_2 is the distance from the lens to the image plane. For a circular aperture of diameter B the PSF is a Bessel function and the width of the Bessel function is the classic resolution limit

$$\Delta x = \frac{1.22 \lambda z_2}{B} = \frac{\lambda_0}{2n \sin \theta} = \frac{\lambda_0}{2 N.A.} \quad \text{where } N.A. = n \sin \theta \text{ (numerical aperture)}$$

We consider the intensity of two points close to each other at the input plane and plot their joint image. (See Figure 11.1). When the two sources are far apart then the two PSF's are clearly separated. But as they get closer it becomes difficult to tell whether we have two sources or a single bigger source. Notice that the relative phase between the two sources makes a difference also. The sidelobes of the PSF can interfere with our ability to see weak sources even farther away than the resolution limit. (See Figure 11.1)

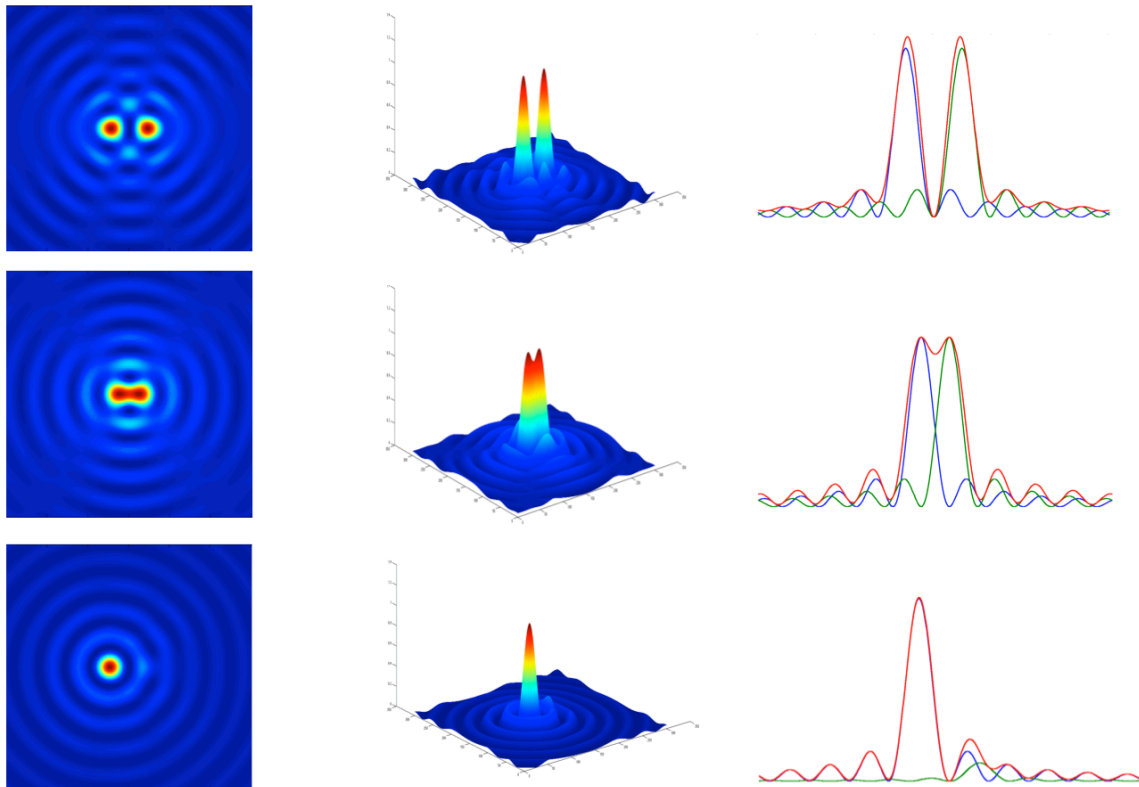


Figure 12.1

We can design a PSF that may have a somewhat broader main lobe but lower sidelobes which can give better image quality. The classic example is a Gaussian PSF. The way this can be accomplished is to have a Gaussian pupil function at the lens rather than the clear aperture we had in the derivation of the previous lecture. Therefore when we take the Fourier transform over x'' we will get a Gaussian (the FT of a Gaussian is a Gaussian) and not a sinc function.

We have been discussing the imaging of 2D objects (thin transparencies placed at the input plane). In fact, objects are generally 3D and therefore it becomes important to think about the 3D PSF of the imaging system. In other words it is important to know the response induced at the image plane as an input point source (scatterer or emitter) moves in z .

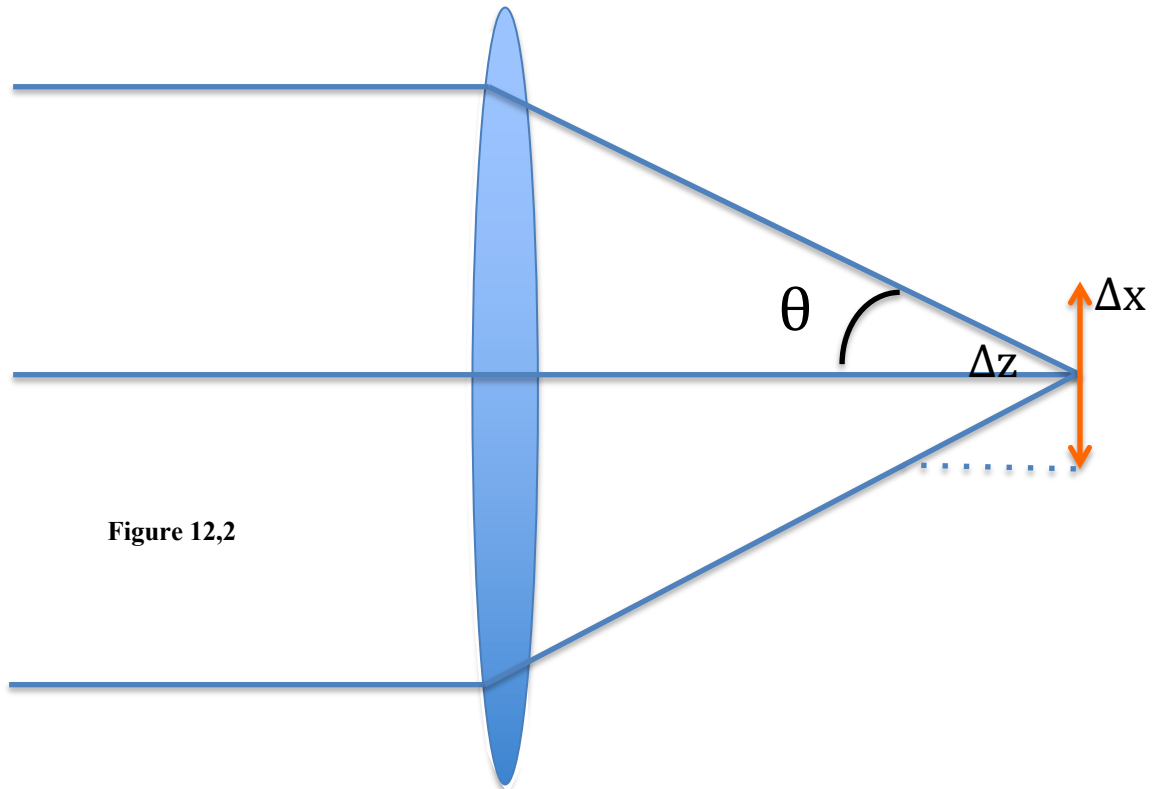


Figure 12,2

As the point source moves from $z=0$ to $z=\Delta z_1$, the focus spot moves to

$$\frac{1}{z_1 - \Delta z_1} + \frac{1}{z'_2} = \frac{1}{F} \Rightarrow z'_2 = \frac{F(z_1 - \Delta z_1)}{z_1 - \Delta z_1 - F} \Rightarrow \Delta z_2 = \frac{-\Delta z_1}{\frac{z_1}{F} - 1}$$

We calculate the 3D PSF by plotting the amplitude of the light as a function of x, y for $z=z_1+z_2+\Delta z_2$. As Δz_2 increases the 2D PSF spreads in the detector plane and the intensity falls off. Just like in the 2D case we can define the resolution criterion somewhat arbitrarily for the distance Δz_2 where the light intensity drops to $\frac{1}{2}$ of the intensity at $\Delta z_2=0$. We can do this numerically using the code for different numerical apertures of the lens. (Figure 11.2). Alternatively we can get an analytical expression by considering either a Gaussian beam coming to a sharp focus in the image plane and then defocussing away from it or by tracing rays. The ray tracing calculation shown in Figure 11.2 is based on the idea that if we ignore diffraction and in the absence of lens aberrations the image of an ideal point source will be an infinitesimally small focus spot. As we move away from the focus, the spot will grow even under the ray optics approximation due to defocussing. We can get an estimate for Δz_2 by calculating the distance in z where the spot size predicted by ray optics will grow to the spot size of the diffraction limit. From the geometry of Figure 11.2 we have:

$$\Delta x = \frac{\lambda_0}{2 NA} \quad \text{where} \quad NA = n \sin \theta \quad \text{and} \quad n = 1 \quad \text{in air}$$

$$\tan \theta = \frac{\Delta x}{\Delta z} \approx \sin \theta \Rightarrow \Delta z = \frac{\Delta x}{\sin \theta} = \frac{\lambda_0}{2 (NA)^2}$$

In other words if the numerical aperture is close to 1 then the transverse and axial resolutions are comparable. Often however in practice the PSF is cigar shaped with the axial resolution being several times poorer than the axial. Exactly the same conclusion is drawn by using the BPM to simulate the focusing of a point source (Gaussian beam) through a lens of finite aperture. The larger aperture gives a tighter focus in x-y (the little red dot) and also a less elongated response in z. In microscopy Δz is the depth resolution of a conventional wide field instrument and we normally want this to be as small as possible. In photography Δz is the depth of focus and generally want this to be as large as possible. If the lens aperture is open wide we obtain good light sensitivity (why?) and better transverse resolution but the objects that are not in the exact plane of best focus are blurred.

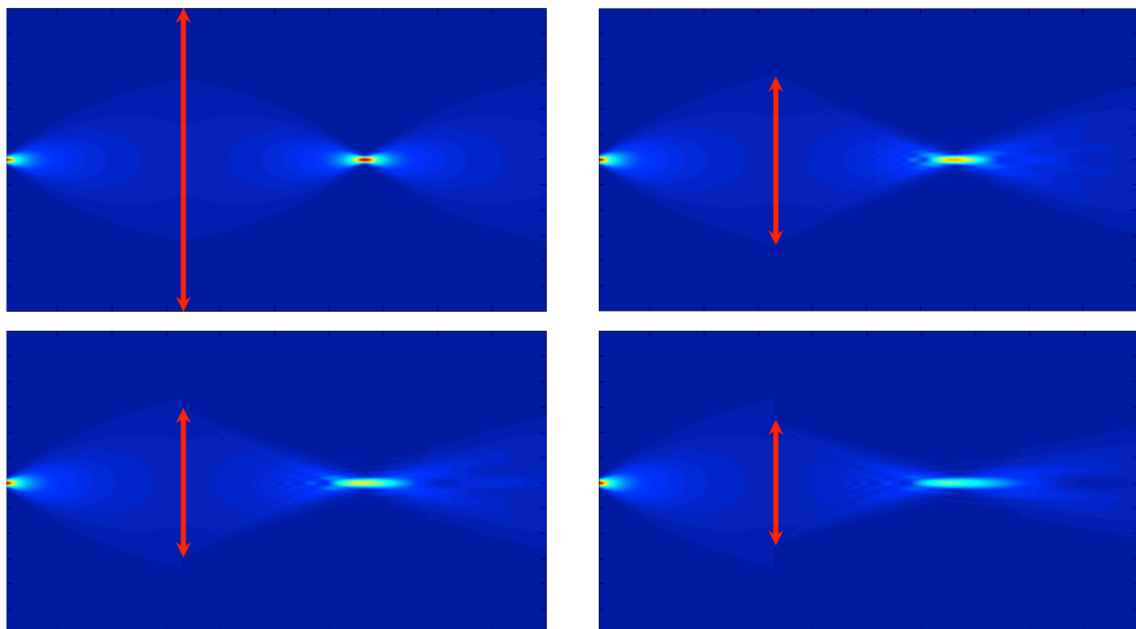


Figure12.3

It is interesting to ask how do we perceive 3D objects. After all we have lenses in our eyes whose aperture opens and closes depending on the brightness of the scene we are looking at. At night the aperture (pupil) opens wide and we lose depth perception, resolution, image quality (abberations become important) and color sensitivity. During the day we normally look at 3D objects that are not transparent. We perceive the 3D shape of the world by focusing in different planes, the parallax between the two eyes, the relative size of the objects, the obstruction of objects that are behind other objects, and the relative motion of objects as we move side-to-side. 3D movies clearly demonstrate dramatically the power of parallax but if we close one eye we still perceive a 3D world even if that eye has an artificial lens that does not automatically refocus. Therefore the brain does a lot of the 3D shape recognition. With a dual lens imaging system or more generally a multiple lens system we can estimate the 3D shape of the object by simple geometry by assuming that each image is a 2D projection of the 2D object in the direction of the optical axis of each imaging system.

Wide field versus scanning microscopy

If the 3D objects to be imaged are partially transparent then things become more complicated. This is often the case in microscopy, particularly when imaging biological samples. We will draw the distinction between wide-field and scanning imaging systems. Wide-field is the type of system we have been discussing so far. The object is illuminated with a beam of light that is large enough to cover the entire object or at least a big part of it. The light transmitted, scattered or emitted by the object is imaged onto a 2D sensor. Alternatively the incident beam can be focused spot that is scanned in 2D or 3D to illuminate sequentially different parts of the object. Clearly the scanning method is more complex and time consuming but it has some advantages. It is easier to explain these advantages assuming the object being imaged is a fluorescent object but the same general arguments apply for scattering objects.

For a wide-field imaging system, as we focus on different planes of the object we get a sharp image of a Δz slice (section) of the object and the rest of the object is recorded as a superimposed blurred background. For complex 3D objects the out of focus planes contribute a background that reduces the contrast. This background grows with object thickness and ultimately it limits our ability to see each slice separately. We can also consider the axial resolution as the separation of two point sources in z that will allow us to clearly distinguish them. The axial resolution is therefore simply $\Delta z = \frac{\lambda}{2(N.A.)^2}$. The basic difference between wide-field imaging

and the scanning version is that the image is obtained by illuminating one voxel (3D pixel) at a time. At first glance it might seem that this gives us an advantage in terms of suppressing the out-of-focus background fluorescence. This is not true however. You can convince yourself of this by considering the time integrated illumination intensity of a scanning beam and compare this to the illumination intensity of the wide-field illumination. They are the same. There is an advantage in terms of resolution in scanning systems since the overall PSF is the product of the PSF of the imaging system that introduces the illuminating beam and the PSF of the imaging system that images the fluorescence onto the 2D sensor. The product of the two PSF's is narrower in all 3 dimensions and therefore there is an improvement in resolution generally by a factor less than 2 ($\sqrt{2}$ for matched Gaussian PSF's).

Confocal Imaging

There are several ways to suppress the background in a scanning imaging system. We will discuss here the confocal microscopy method, invented by Marvin Minsky (better known as the father of the field of artificial intelligence). The image on the left in Figure 11.4 was obtained with a wide-field microscope by focusing on the fluorescence emitted by a cell. Also shown in Figure 11.4 is the same cell imaged with a "confocal" microscope. The improvement provided by the confocal microscope is evident.

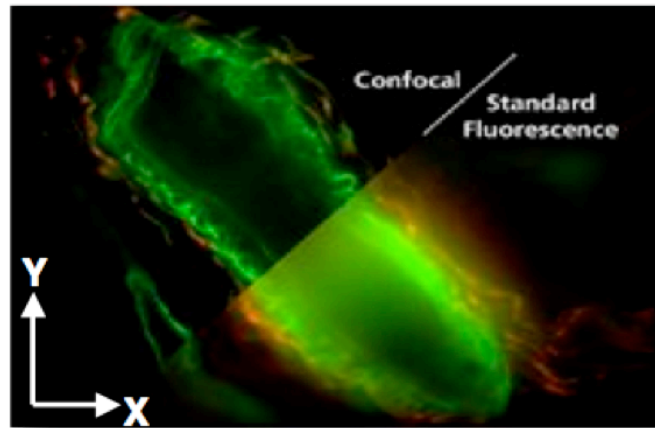


Figure 12.4

The optical arrangement of confocal microscope is shown in Figure 11.5.

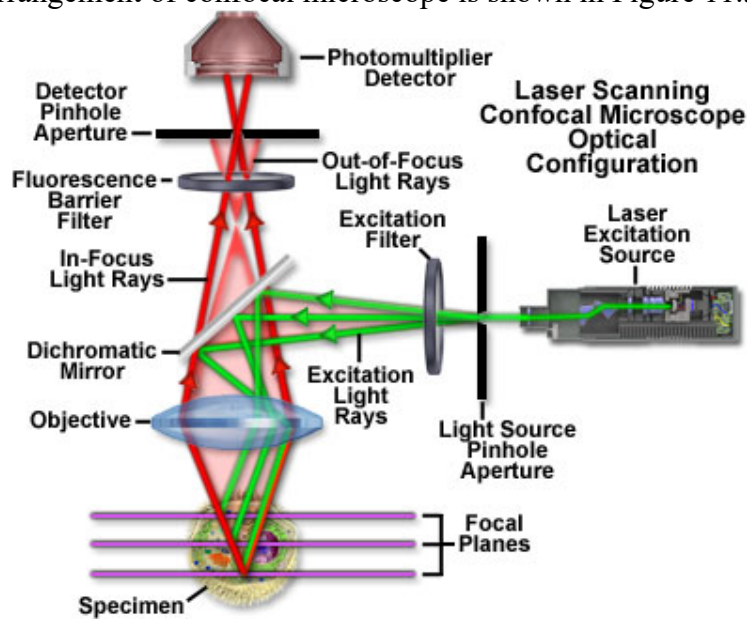


Figure 12.5

The illuminating laser is focused on the object (if a non-laser source is used then a pinhole is imaged onto the object instead). The object is mounted on a 3D translational stage so that the illuminating spot can be sequentially scanned throughout the volume of the object. The fluorescence is not uniform throughout the volume of the object but it is much stronger in the region near the focus. This illumination volume is approximately the same as the cigar-shaped 3D PSF of the imaging system.

The fluorescence generated is imaged onto the plane of the “pinhole aperture”. The combined PSF of the two imaging systems determined the resolution as we discussed earlier. The difference between the two PSF’s is shown in Figure 11.6. The difference is evident and the resulting difference in the quality of the wide-field versus scanning imaging can be significant. The dramatic improvement observed in Figure 11.4 is due to the pinhole however. Light that is emitted (or scattered) from a point source located at the plane of the object that is not in focus with respect to the plane of the pinhole aperture will be blurred and spread to a bigger diameter compared to the pinhole size. Points at the plane of best focus will be mapped to a diffraction limited spot. The

pinhole diameter is generally selected to be equal to the diffraction limited resolution, thereby passing efficiently the light originating from the *confocal* position on the object. Points on the object that are not in focus spread out on the plane of the pinhole and are blocked. Therefore the out-of-focus planes of the object are suppressed and they do not introduce the unwanted background.

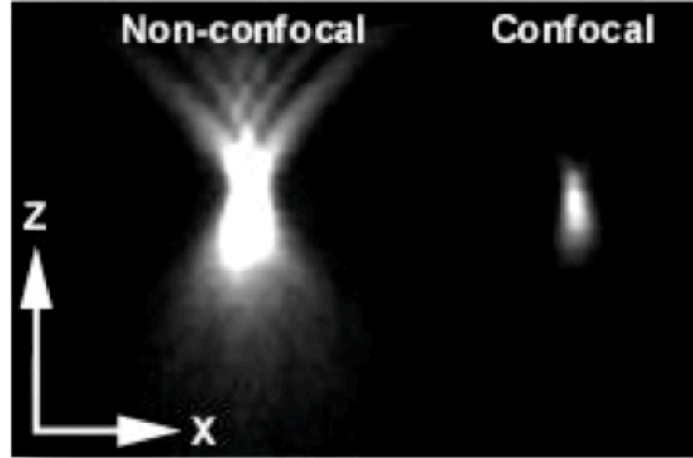


Figure 12.6

Tomography

Wide field Microscopy

Imaging of 3D objects is often referred to as sectioning in microscopy. In a conventional wide field microscope the projection of the 3D object in the direction of the optical axis is obtained (see Figure 1). Under the ray optics approximation (diffraction can be neglected) the signal $d(x, y)$ detected on the imaging sensor, in the wide field microscope is

$$d(x, y) = \left| e^{-\int \alpha(x, y, z) dz} e^{-j \int \beta(x, y, z) dz} e^{-jkz} \right|^2 = e^{-2 \int \alpha(x, y, z) dz} \quad (1.1)$$

where $f(x, y, z) = e^{-\alpha(x, y, z)} e^{j\phi(x, y, z)}$ is the complex, 3D transmittance function of the object. It is as if the object behaved like a thin transparency except the z dependence of the absorption and the dielectric constant are explicitly taken into account. The function $\alpha(x, y, z)$ describes the 3D absorbtance of the sample whereas the 3D distribution of the index of refraction is proportional to $\phi(x, y, z)$. Notice that in the absence of a detection method that records the phase the detected signal does not contain information about the index of refraction in this case. More on this later.

Radon Transform

If we illuminate the object with a plane wave at an angle (θ_x, θ_y) we can calculate the detected signal by rotating the coordinates system and Eq. (1.1) can be rewritten in the rotated coordinate system.

Diffraction Tomography

If diffraction cannot be neglected we can use the Fresnel integral to calculate $d(x,y)$ assuming the sample is illuminated with a plane wave propagating with amplitude A propagating along the z axis :

$$d(x,y) = \left| \int \frac{e^{-jk(z-z')}}{j\lambda(z-z')} \iint f(x',y',z') A e^{-jkz'} e^{-j\frac{\pi}{\lambda(z-z')}[(x-x')^2+(y-y')^2]} dx' dy' dz' \right|^2 \quad (1.2)$$

$$\approx \frac{e^{-jkz}}{j\lambda} \left[f A e^{-jkz'} \otimes_{3D} \frac{e^{-jkr}}{r} \right]$$

where $z=0$ is at the focal plane of the imaging system in Figure 1.

The above expression has two approximations: The first is the usual approximations for the Fresnel integral (paraxial, scalar diffraction) which we undid by replacing the paraxial version with the spherical wave and the second is the Born approximation where we have implicitly neglected multiple scattering by assuming that the Fresnel formula which is applicable for propagation in homogeneous media can be used. If we don't use the paraxial approximation and use the scattering cross section, Eq. 1.2 becomes the Born approximation diffraction integral. If the incident field is not a plane wave along z or is not even a plane wave at all then if we neglect the modification of the incident wave as it propagates through the object then we can simply replace A by the Fresnel diffraction integral of the incident wave accounting for its propagation from $z = 0$ to $z = z'$. We will come back go this later but first we will explore how this is done in the Fourier plane.

The Wolf transform

The illumination pattern is decomposed into its Fourier components and we can consider the light scattered by the 3D sample for each plane wave component at a time. WE also take the 3D Fourier transform of the transmittance function $f(x,y,z)$ decomposing it into gratings of varying magnitude and orientation. From our analysis of the diffraction of volume gratings when illuminated by a plane wave we know that there is a Bragg condition relating the incidence angle θ of the illumination, the period of the volume grating Λ and its orientation. This Bragg matching condition is depicted diagrammatically in Figure 12.7.

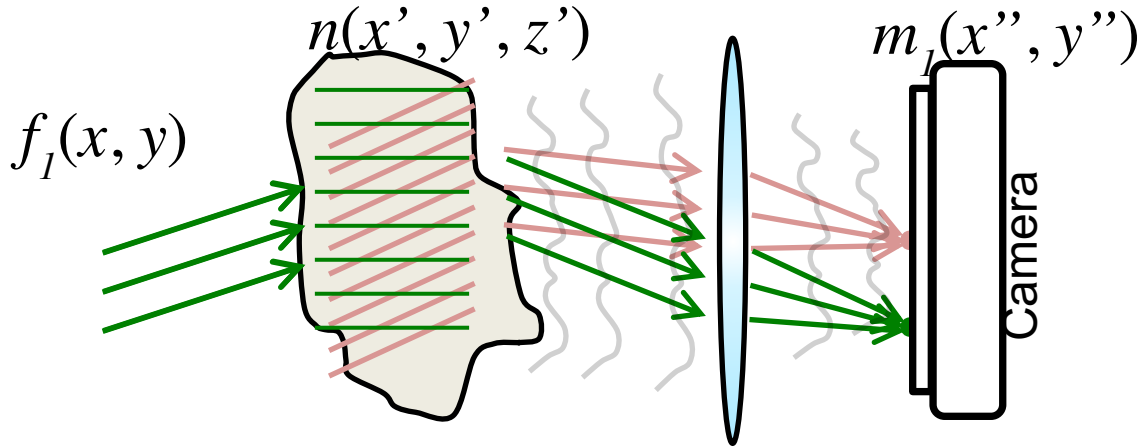


Figure 12.7

If we know the amplitude and phase of the illuminating wave, then we can derive the diffracted field due to each individual grating component of the object. We have seen that for a thick grating the diffracted wave is approximately a plane with a wave-vector $\vec{k} = \vec{k}_{inc} - \vec{K}$ with the constraint that both \vec{k} and \vec{k}_{inc} lie on the Ewald sphere. In the optical system of Figure X, \vec{k} is focused onto a pixel of the camera determined by the transverse components k_x and k_y . Specifically $x'' = u\lambda F = k_x \lambda F / 2\pi$ and $y'' = v\lambda F / 2\pi = k_y \lambda F / 2\pi$

The amplitude and phase of the light incident on each pixel of the camera is a measure of the amplitude and phase of the corresponding grating component of the object with 3D spatial frequency components

$$\vec{K} = \begin{pmatrix} K_x \\ K_y \\ K_z \end{pmatrix} = \begin{pmatrix} k_{xinc} - k_x \\ k_{yinc} - k_y \\ \sqrt{k^2 - k_{xinc}^2 - k_{yinc}^2} - \sqrt{k^2 - k_x^2 - k_y^2} \end{pmatrix}$$

For each measurement of the camera the number of gratings we measure is equal to the number of gratings on the camera. Changing the angle of hthan 10^6 pixels and it is possible to have more than 10^3 illumination angles, yielding measurement of the amplitude and phase of more than a billion frequency components (gratings) of the 3D Fourier spectrum of the object. An inverse 3D Fourier transform of this measured portion of the spectrum yields the estimate of the object $f(x,y,z)$.

For the BPM approach to Optical Diffraction Tomography see the following paper:

<https://www.osapublishing.org/optica/abstract.cfm?uri=optica-2-6-517>